International Journal of Remote Sensing
Vol. 28, No. 12, 20 June 2007, 2645–2670

The Nightsat mission concept

C. D. ELVIDGE*†, P. CINZANO‡§, D. R. PETTIT¶, J. ARVESEN**, P. SUTTON††, C. SMALL‡‡, R. NEMANI§§, T. LONGCORE¶¶‖‖, C. RICH¶¶, J. SAFRAN†††, J. WEEKS‡‡‡ and S. EBENER§§§

†Earth Observation Group, NOAA-NESDIS National Geophysical Data Center, Boulder, Colorado 80305, USA

‡Dipartimento di Astronomia, Università di Padova, Padova 2-35122, Italy

§Istituto di Scienza e Tecnologia dell'Inquinamento Luminoso (ISTIL), Thiene 13-36016, Italy

¶NASA Johnson Spaceflight Center, Houston, Texas 77058, USA

**Cirrus Digital Systems, Tiburon, California 94920, USA

††Department of Geography, University of Denver, Denver, Colorado 80208, USA; Department of Geography, Population and Environmental Management, Flinders University, Adelaide, Australia

‡‡Lamont-Doherty Earth Observatory of Columbia University, Palisades, New York 10964-8000, USA

§§NASA Ames Research Center, Moffett Field, California 94035, USA

¶¶The Urban Wildlands Group, P.O. Box 24020, Los Angeles, California 90024-0020, USA

‖‖Department of Geography, University of Southern California, Los Angeles, California 90089-0255, USA

†††Cooperative Institute for Research in the Environmental Sciences, University of Colorado 80309, USA

‡‡‡International Population Center, San Diego State University, San Diego, California 92182, USA

§§§World Health Organization, CH-1271 Geneva 27, Switzerland

(*Received 14 November 2005; in final form 27 August 2006*)

Nightsat is a concept for a satellite system capable of global observation of the location, extent and brightness of night-time lights at a spatial resolution suitable for the delineation of primary features within human settlements. Based on requirements from several fields of scientific inquiry, Nightsat should be capable of producing a complete cloud-free global map of lights on an annual basis. We have used a combination of high-resolution field spectra of outdoor lighting, moderate resolution colour photography of cities at night from the International Space Station, and high-resolution airborne camera imagery acquired at night to define a range of spatial, spectral, and detection limit options for a future Nightsat mission. The primary findings of our study are that Nightsat should collect data from a near-synchronous orbit in the early evening with 50 to 100 m spatial resolution and have detection limits of $2.5E^{-8}$ Watts $cm^{-2}sr^{-1}\mu m^{-1}$ or better. Although panchromatic low-light imaging data would be useful, multispectral low-light imaging data would provide valuable information on

*Corresponding author. Email: Chris.Elvidge@noaa.gov

International Journal of Remote Sensing
ISSN 0143-1161 print/ISSN 1366-5901 online
http://www.tandf.co.uk/journals
DOI: 10.1080/01431160600981525

the type or character of lighting; potentially stronger predictors of variables, such as ambient population density and economic activity; and valuable information to predict response of other species to artificial night lighting. The Nightsat mission concept is unique in its focus on observing a human activity, in contrast to traditional Earth observing systems that focus on natural systems.

1. Introduction

Nocturnal lighting is a unique indicator of human activity that can be measured from space. A new satellite sensor for night-time lighting, Nightsat, could be used to map the extent and character of development more accurately and completely than most currently available tools. Improved global mapping of human settlements and human activity would address a variety of science and policy issues in the 21st century—an era in which human population numbers are expected grow substantially from the current 6+ billion mark.

The density of infrastructure and the intensity of human activity—or 'urbanness'—can be viewed as a continuum, ranging from wilderness at one extreme to central business districts at the other extreme (Weeks 2004, Weeks *et al.* in press). Human beings worldwide tend to cluster in spatially limited habitats, occupying less than 5% of the world's land area. Today, more than half of the world's population lives in urban areas, with the most rapid increases occurring in the developing countries of Latin America, Asia and Africa. In Europe, North America and Japan 80% or more of the population already live in urban areas. Worldwide, the trend is for increasing numbers of people to concentrate in settlements and for the settlements to expand at their perimeters. Sprawl on the urban fringe and exurban development are two of the more conspicuous signs of urban change, but structural change permeates urban areas through continuous re-development and the replacement of ageing infrastucture with new construction. Thus, urban areas are in a constant state of re-development and flux that reflect both, growing urban populations and the evolution of urbanizing technologies.

Interest in satellite remote sensing of nocturnal lighting stems, in part, from the difficulty in global mapping of human settlements in a repeatable, timely manner from traditional sources. Although development features can be extracted from high spatial resolution (~1 m) satellite imagery, the production of global annual maps of development from these data sources is not feasible (at this time) from either a collection or analysis perspective. Moderate resolution Landsat-style systems offer the potential of global collections on an annual basis and such data have been used effectively for mapping urban areas and tracking growth in local settings. Recent analyses of Landsat data from diverse urban areas worldwide indicate, however, that the combination of inter-urban and intra-urban heterogeneity precludes the existence of any unique spectral characteristic of urban areas as a thematic class (Small 2005). The spectral complexity and classification ambiguities of Landsat-style data contribute to the lengthy production period typical for continental to global-scale derived products from these sources. For example, both the USGS National Land Cover Data (NLCD) for the USA (Vogelmann *et al.* 2001) and NASA's global Geocover Land Cover products required five years to complete. In addition, Landsat-style data are poorly suited for the detection of sparse development.

In contrast, the remote sensing of nocturnal lighting provides an accurate, economical, and straightforward way to map the global distribution and density of developed areas. The widespread use of outdoor lighting is a relatively recent

phenomenon, tracing its roots back to the electric light bulb, commercialized by Thomas Edison in the early 1880s. Nocturnal lighting has emerged as one of the hallmarks of modern development and provides a unique attribute for identifying the presence of development or human activity that can be sensed remotely. Although there are some cultural variations in the quantity and quality of lighting in various countries, there is a remarkable level of similarity in lighting technology and lighting levels around the world. The primary factor affecting the quantity of lighting is wealth. Regions with high per capita income have much more lighting than regions with low per capita income. Even within affluent regions, however, lighting technology (lamps and lighting fixtures) is gradually changing, as pressure is applied to reduce night-time sky brightness and conserve energy. In some applications, night-time lights are used as a proxy for variables that are difficult to measure in a globally consistent manner, including many socio-economic variables, such as population density and gross domestic product (e.g. Doll *et al.* 2000, Balk *et al.* 2005). In other applications, the spatial distribution and quality of lighting is used as a variable directly, as in the detection of bioluminescence (Miller *et al.* 2005) and analyses of ecological effects of nocturnal lighting (see chapters in Rich and Longcore 2006), the analysis of artificial sky brightness impacts on the visibility of stars and planets, and human health effects of lighting (Hansen 2001, Pauley 2004, Stevens and Rea 2001).

The only satellite sensor currently collecting global night-time lights data is the U.S. Air Force Defense Meteorological Satellite Program (DMSP) Operational Linescan System (OLS). The NOAA National Geophysical Data Center (NGDC) has been producing DMSP night-time lights products since 1994 and has worked extensively with the scientific community to develop applications for this data source. As a result of these efforts, it can be concluded that the current technology for global mapping of night-time lights falls short of the science community's requirements. The objective of this paper is to review the science community's requirements for global satellite observations of nocturnal lighting and to define a Nightsat mission concept to address these requirements. Most of the scientific applications for satellite-observed night-time lights could be addressed by a system capable of producing an annual cloud-free night-time lights composite that is radiance calibrated and collected in spectral bands that are linked to standards used in lighting technology.

2. Current status

Since the early 1970s the U.S. Air Force Defense Meteorological Satellite Program has operated polar orbiting platforms, carrying cloud imaging satellite sensors capable of detecting clouds using two broad spectral bands: visible–near infrared (VNIR) and thermal infrared (TIR). The program began with the SAP (sensor aerospace vehicle electronics package), which were flown from 1970–76. The current generation of OLS sensors began flying in 1976 and are expected to continue flying until at least 2010. At night, the VNIR band is intensified with a photomultiplier tube to permit detection of clouds illuminated by moonlight. The OLS detects radiances down to the $5E^{-10}$ Watts $cm^{-2}sr^{-1}$ range (Table 1), which makes it possible to detect artificial sky brightness surrounding large cities and gas flares.

A digital archive for the DMSP–OLS data was established in mid-1992 at NGDC. In 1994, NGDC began developing algorithms for producing annual global cloud-

Table 1. Comparison of the low-light imaging systems surveyed.

Sensor	Years	Description	Platform	Altitude	Ground sample distance	Detection limit
Operational Linescan System (OLS)	1973–present	Scanning telescope with three single detector focal planes. Light intensification achieved with a photomultiplier tube (PMT).	Defense Meteorological Satellite Program (DMSP)	830 km	2.7 km	10^{-9} watts $cm^{-2}\,sr^{-1}$
Visible Infrared Imaging Radiometer Suite (VIIRS)	2009+	Twenty-two channel imaging radiometer with a single broad low-light imaging band employing time-delay integration (TDI) on a charge-coupled device (CCD).	National Polar-orbiting Operational Environmental Satellite System (NPOESS)	830 km	742 m	10^{-9} watts $cm^{-2}\,sr^{-1}$
Kodak-Nikon 760	2002–2003	Colour digital camera with image motion compensation device.	International Space Station (ISS)	390 km	60–100 m	Unknown
Cirrus DCS	2004	Colour digital camera (Hasselblad 555ELD with Kodak DCS ProBack with IR blocking filter removed).	NASA ER-2	14 km	1.5 m	10^{-5} watts $cm^{-2}\,sr^{-1}$

free composites of night-time lights using DMSP data (Elvidge *et al.* 1997a, 1999, 2001). These annual products have been used for a variety of applications, including:

(a) spatial modelling of socio-economic variables, such as population density (Dobson *et al.* 2000, Sutton 1997 and 2003, Sutton *et al.*, 1997, 2001, 2003, Balk *et al.* 2005) and economic activity (Elvidge *et al.* 1997b, Doll *et al.* 2000, Ebener *et al.* 2005);
(b) measurements of the density of infrastructure (Elvidge *et al.* 2004) for use in hydrologic modelling, flood prediction, the assessment of losses in agricultural land (Imhoff *et al.* 1997), terrestrial carbon dynamics (Milesi *et al.* 2003 and 2005, Imhoff *et al.* 2004);
(c) as reference data in the detection of power outages following disasters (Elvidge *et al.* 1998);
(d) analysis of the ecological effects of nocturnal lighting on sea turtle hatchlings (Salmon *et al.* 2000 and Salmon 2006);
(e) inventory of heavily lit fishing boats (Cho *et al.* 1999, Rodhouse *et al.* 2001, Waluda *et al.* 2002, Maxwell *et al.*, 2004);
(f) estimation of artificial sky brightness and its effect on the visibility of astronomical features (Cinzano *et al.* 2000, 2001a, 2001b, 2004);
(g) calculation of anthropogenic emissions to the atmosphere (Saxon *et al.* 1997 and Toenges-Schuller *et al.* 2006).

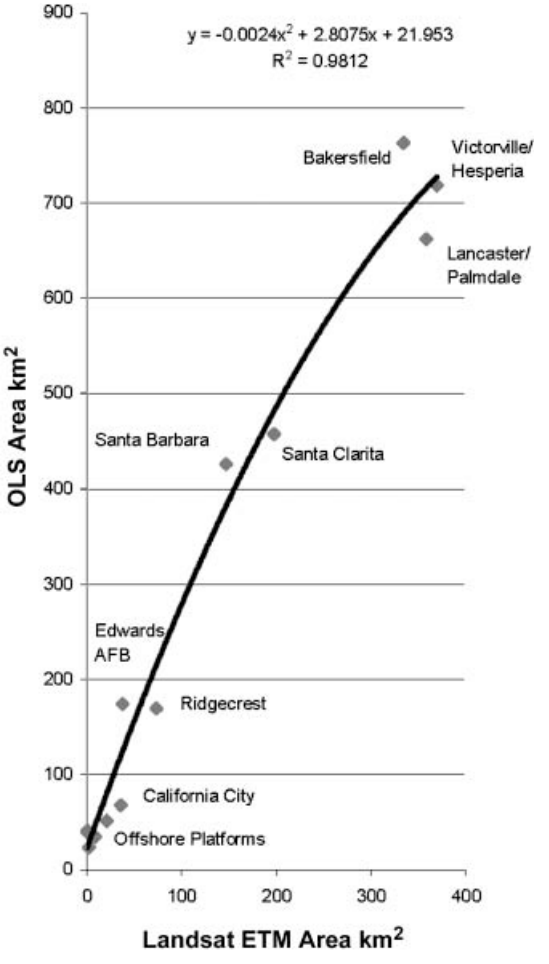

Figure 1. The area of lights measured by DMSP–OLS versus the area of the corresponding light sources derived from Landsat ETM+ data. Spatial extents of both the OLS lights and developments observed in the Landsat data were extracted visually.

In working with the science community using the annual composites of DMSP night-time lights, certain characteristics of the products were identified that limited the utility of the data. The OLS generates low-light imaging data with a 2.7-km ground sample distance and the ground instantaneous field of view at nadir is approximately 5 km. As a consequence of the coarse spatial resolution and the accumulation of geolocation errors in the compositing process, the OLS-derived night-time lights cover much larger areas than the lit areas on the ground (figure 1 and Small *et al.* 2005). In addition, the scattering of light in the atmosphere and the photomultiplier's response to bright emission sources results in an 'overglow' effect in OLS night-time lights. This overglow is conspicuous at gas flares and offshore from major urban centres (figure 2). Higher spatial resolution would be required to unambiguously separate the spatially diffused overglow arising from artificial sky brightness from lighting emitted directly from development present on the ground. Additionally, the DMSP lights cannot be used to analyse differences in lighting type

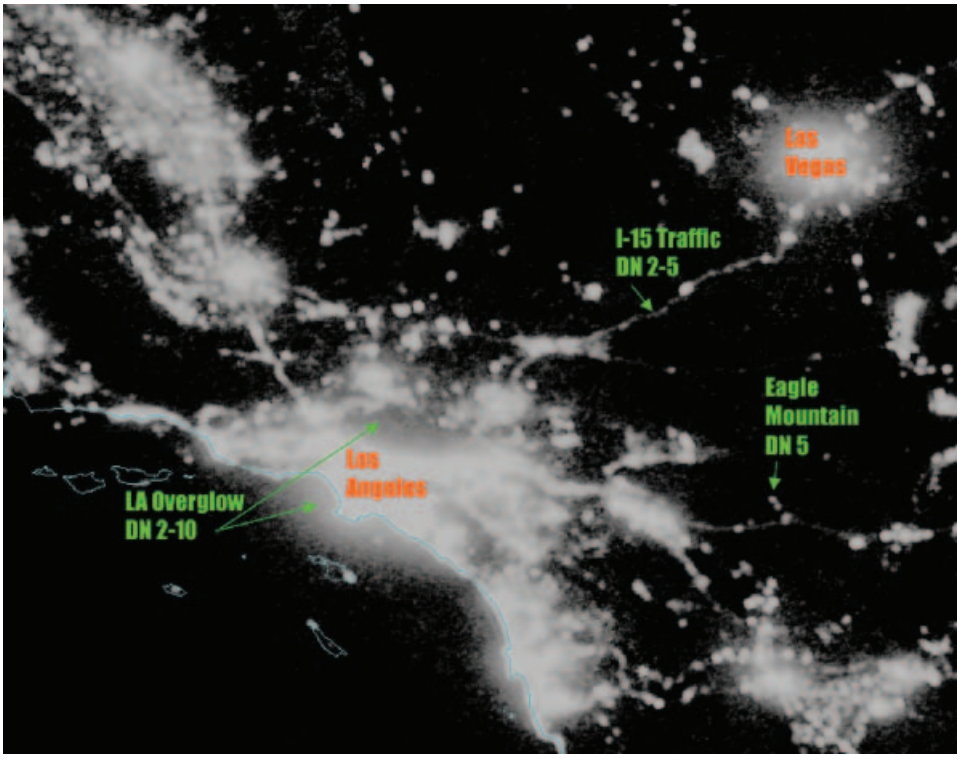

Figure 2. DMSP-OLS cloud-free composite of 2003 night-time lights contrast enhanced to show the overglow surrounding bright urban centres. The overglow arises from artificial sky brightness and extends more than 50 km offshore from Los Angeles, California and blankets the San Gabriel Mountains north of Los Angeles. Overglow digital number (DN) values exceed DN values for lighting from Interstate 15 highway traffic and many small towns.

or to discriminate sub-kilometer variations in lighting, are typically saturated in urban centres, and have uncertain radiometry.

Based on these results, eleven specific shortcomings for the observation of night-time lights have been identified for the OLS sensor: (a) coarse spatial resolution; (b) lack of on-board calibration; (c) lack of systematic recording of in-flight gain changes; (d) limited dynamic range; (e) six-bit quantitization; (f) signal saturation in urban centres resulting from standard operation at the high gain setting; (g) lack of a thermal band suitable for fire detection; (h) limited data recording and download capabilities (most OLS data are averaged on-board to enable download of global coverage); (i) lack of a well characterized point spread function (PSF); (j) lack of a well characterized field-of-view (FOV); and (k) lack of multiple spectral bands capable of detecting lights.

The follow-on for the OLS is the visible/infrared imager/radiometer suite (VIIRS), which will fly on the national polar-orbiting operational environmental satellite system (NPOESS). The first VIIRS is currently being built and represents an improved (table 1), but still imperfect, instrument to measure nocturnal lighting (Lee *et al.* 2004). The NPOESS VIIRS instrument will provide low-light imaging data with improved spatial resolution (0.742 km), wider dynamic range, higher quantitization, on-board calibration, and simultaneous observation with a broader suite of bands for improved cloud and fire discrimination over the OLS. The VIIRS is not, however, designed with

the objective of sensing night-time lights. Rather, it has the objective of night-time visible band imaging of moonlit clouds—the same mission objective of the OLS low-light imaging. While the VIIRS will acquire improved night-time lighting data, it is not optimal for this application. In particular, the VIIRS low-light imaging spatial resolution will be too coarse to permit the observation of key night-time lighting features within human settlements and the spectral band to be used for the low-light imaging is not tailored for night-time lighting.

3. Observational requirements

The environmental and social science applications described above have a substantial overlap in their night-time lights product requirements. Thus, a suite of product types can be defined that satisfy multiple user communities. The largest numbers of potential users are those focused on human settlements. Below is a listing of a basic product suite for human settlements that could potentially be derived from night-time lights. Because of the rapid changes ongoing in human settlements worldwide, these key global datasets would ideally be updated annually with a product latency of not more than one year for measurement of the rates of change and annual growth increments.

(1) Products depicting the geographic "footprints" of human settlements of all sizes. This includes the outline of the developed areas and specific estimates of constructed area.
(2) Location and extent of sparse development in rural areas.
(3) Identification of intra-urban classes, such as residential areas, commercial and industrial areas, and open lands with little or no development present.
(4) Vectors for streets and roads.

Our assessment is that a low light imaging system optimized for deriving the listed human settlement products would generate data suitable for a wider range of applications, such as monitoring fishing boat activity, mapping the spatial distribution of economic activity, or the analysis of ecological effects of nocturnal lighting (Rich and Longcore 2006). The low-light imaging spectral, radiometric and spatial resolution requirements for the extraction of the features listed above have not been defined to date.

4. Data collection

To explore the remote sensing of night-time lights, we have collected data on the ground, from the air, and from space.

4.1 *Field spectra of lights*

A survey of the spectral information content of commonly used lighting sources was conducted using high spectral resolution field spectra. Spectra were acquired of a suite of outdoor lighting types, including streetlights (mercury vapour lamps and high pressure sodium vapour lamps), incandescent lights from vehicles and homes, and lights present at commercial and government facilities (fluorescent, neon and low-pressure sodium vapour lamps). Spectra were acquired using a portable spectrometer manufactured by analytical spectral devices. The spectra were collected as irradiances, while pointing the instrument head directly at each light source.

4.2 *Space photography*

We investigated the feature content of moderate-resolution colour imagery of lights at night from space with digital photography acquired from the International Space Station (ISS). Astronauts have long marveled at the shear beauty and the technical information about the development of humanity from city lights at night as viewed from orbit. However, the features have been difficult to photograph, owing to mismatches between the optimal exposure times and the velocity of the spacecraft. During Expedition 6 (23 November 2002—3 May 2003) to the International Space Station, a mechanized but manually driven image motion compensation mount was built from existing hardware and images were acquired of cities at night all over the world through an optical-quality nadir-viewing window. Images were acquired of large urban areas and a number of sparsely populated areas. About 2000 images with dark currents and flat field exposures were collected.

The orbital tracking mount consisted of the IMAX movie camera mount with both, a 70 mm film format (55 mm square image) Haselblad 203 camera with 350mm telephoto lens (a square field of view of 9 degrees) and a Kodak-Nikon 760 digital camera with 58 mm, f1.2 nocto aspheric lens (see figure 3). A Makita drill driver was used to rotate a long threaded bolt that pushed against a wedge and drove one direction of gimbal at a smooth rate, determined by the degree that the trigger was squeezed on the drill driver. The mount was attached to the 508 cm diameter, nadir viewing science window in the US Laboratory module so that the direction of gimbal was aligned with the direction of orbital motion. In operation, the astronaut would look through the Hasselblad camera, vary the rotation rate of the drill driver until city lights were stationary with respect to the view finder reticule, and then take the images using the Kodak-Nikon 760 digital camera. The ground sample distance (GSD) of the imagery is 60 m, however not all the images had the same degree of sharpness, hence ground resolution owing to variations in effectiveness of the image motion compensation.

4.3 *Airborne photography*

The spatial resolution and detection limit requirements for a Nightsat were investigated using night-time visible band digital imagery, acquired using a Cirrus DSC camera (table 1). The Cirrus camera was flown on NASA's ER-2 aircraft across Las Vegas, Nevada and Los Angeles, California on 27 September 2004 at 13.7 km above sea level. Digital photography was acquired using an 80 mm lens and a 1/60th s exposure. The Cirrus DCS is designed as a colour camera. For the night-time collections the infrared blocking filter was removed and the signal from each of the three bands were aggregated in post flight processing to form panchromatic imagery. The collections span desert areas devoid of lighting, cross a wide range of development types, and encounter the world's brightest light, emitted from the Luxor Hotel and Casino in Las Vegas. The Luxor lighting installation is composed of thirty-nine 7000 Watt xenon lamps, pointing straight up into the sky (figure 4). The lighting installation intensity reaches 40 billion candelas. The spatial resolution of the Cirrus camera data was 1.5 m at 16-bit quantitization. The Cirrus camera was subsequently calibrated using an integrating sphere at the NASA Ames Research Center.

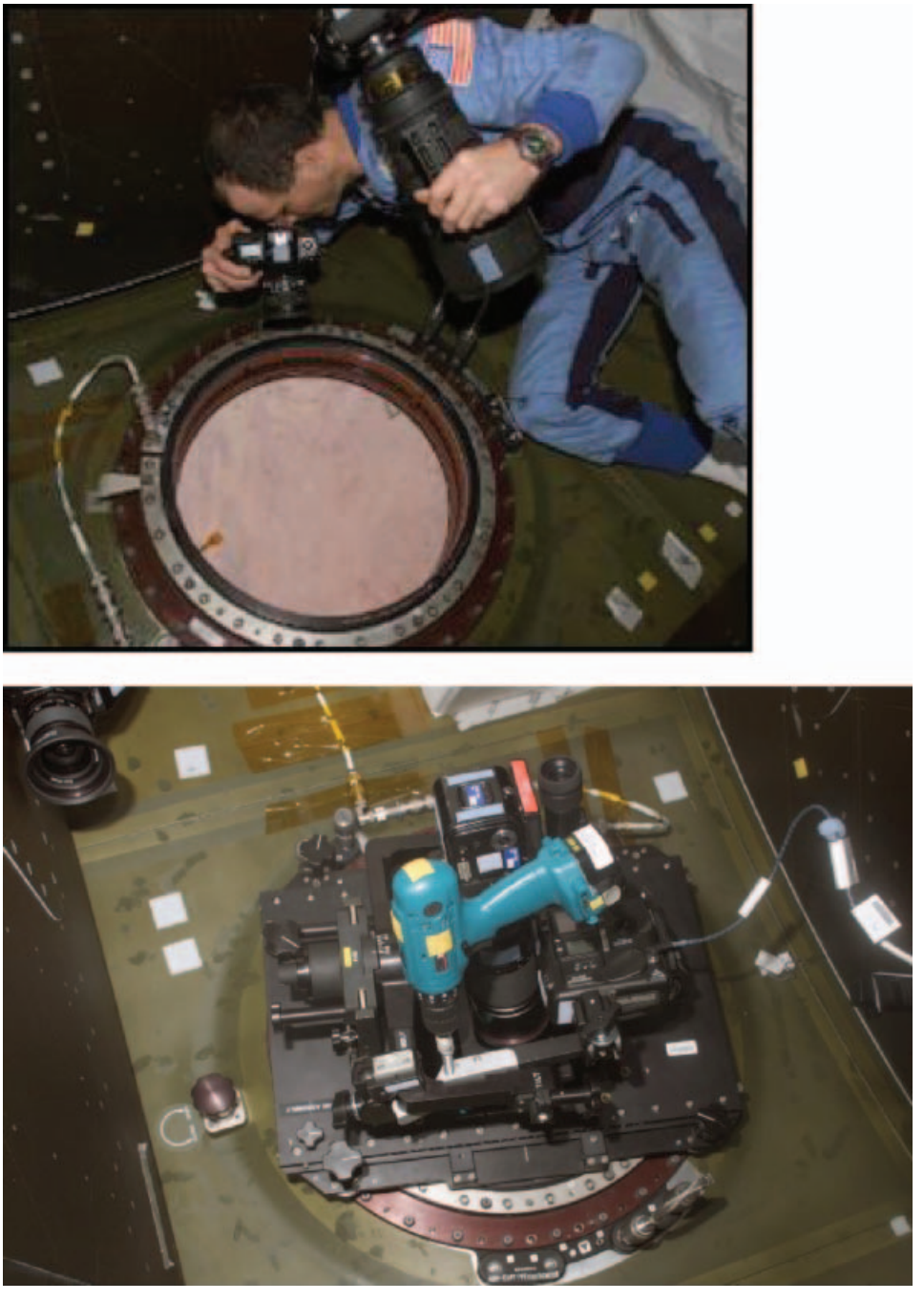

Figure 3. The optical window on the International Space Station and the improvized image motion compensation attachment used to acquire moderate resolution colour photography of cities at night.

Figure 4. The 40 billion candela xenon beacon pointed into the sky from the Luxor Hotel and Casino in Las Vegas, Nevada was one of several light sources found to saturate the Cirrus DCS camera flown at 13.7 km above the earth.

5. Defining requirements for Nightsat data

5.1 *Spatial resolution requirements*

To determine the spatial resolution necessary to adequately characterize night-time lights we analysed the 1.5 m resolution night-time camera imagery. In the full resolution imagery it is easy to distinguish major roads, commercial centres, dimly lit residential neighbourhoods, and undeveloped tracts without lights (figure 5). Acceptable spatial resolutions would retain these basic features. We used the 1.5 m data to simulate imagery at resolutions of 25, 50, 100, 200 and 742 m (figure 6). In addition, we examined the ISS night-time photography of cities at night. Figure 7 shows two of the ISS images we examined, covering Chicago and Tokyo.

With the original Cirrus camera data (1.5 m resolution), it is possible to detect many individual lights in residential neighbourhoods, individual streetlights and a lit area surrounding many of these lights. Lines of streetlights delineate many streets and roads. Commercial buildings and commercial properties are lit much more brightly than residential areas and can be readily distinguished. As the resolution is degraded, finer detail is gradually lost, but most features, such as streets and roads, are still evident at both 25 and 50 m resolution. At 100 m resolution, major forms are still evident, such as major streets and roads and clusters of commercial buildings. At 200 m resolution, very few features remain. At 742 m resolution, the resolution that will be provided by the VIIRS low-light imaging band, none of the features seen so clearly in the original imagery can be discerned.

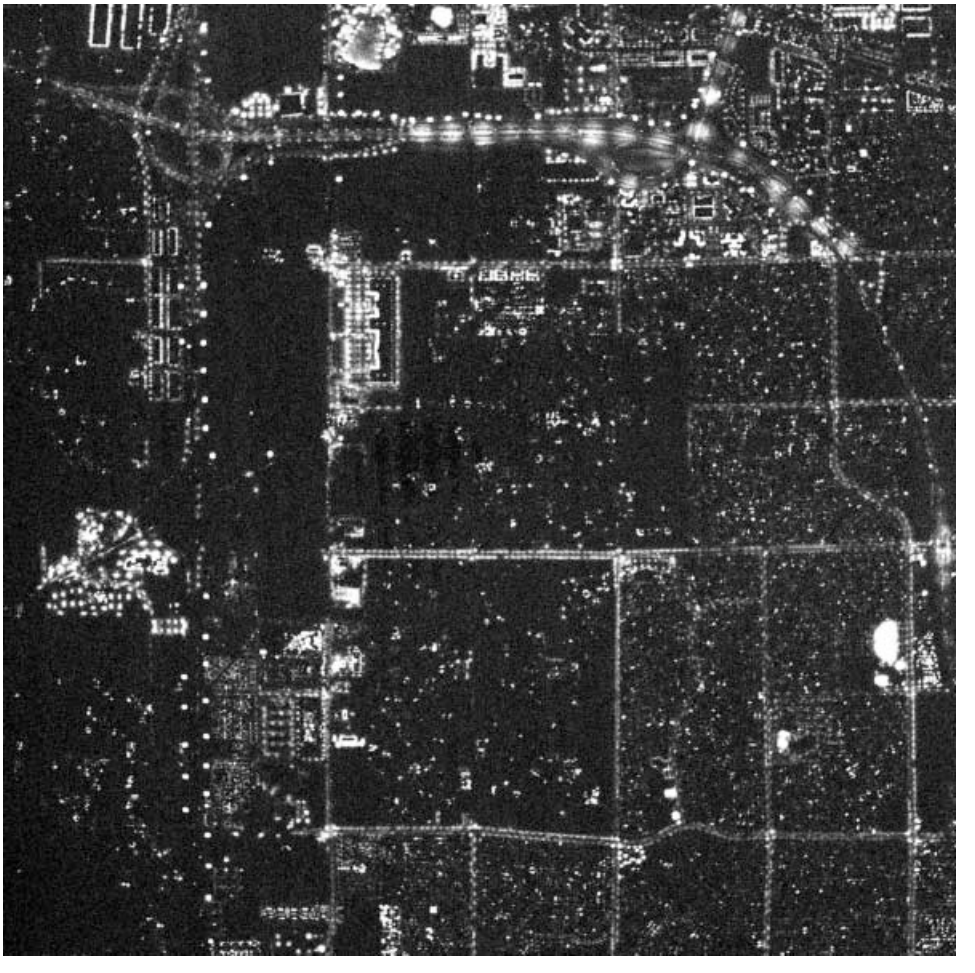

Figure 5. Airborne night-time lights imagery at 1.5 m resolution covering a portion of Las Vegas, Nevada. Imagery acquired from NASA's ER-2 flown at 13.7 km above the Earth with a Cirrus DCS digital camera.

Based on the spatial resolution simulations conducted with the Cirrus camera imagery, we conclude that 50 to 100 m resolution would be necessary to retain the primary night-time lights features present in urban and rural environments. These findings are corroborated by the delineation of commercial centres and major roads with the ~60 m resolution ISS night-time photography (figure 7). Obviously, a sensor capable of acquiring 25 m low-light imaging data will be physically larger, more expensive, and have a higher data volume than a system providing 100 m resolution data. Overall, 50 to 60 m resolution low-light imaging data appears to strike the best balance, making it feasible to map urban forms and measure development growth rates on an annual basis.

5.2 *Low-light imaging spectral bands*

Outdoor lighting sources can be divided into three primary types: flames (light produced by combustion), incandescent (light produced using heated filaments), and vapour lamps (where light is generated by electrically charged gases, e.g. mercury

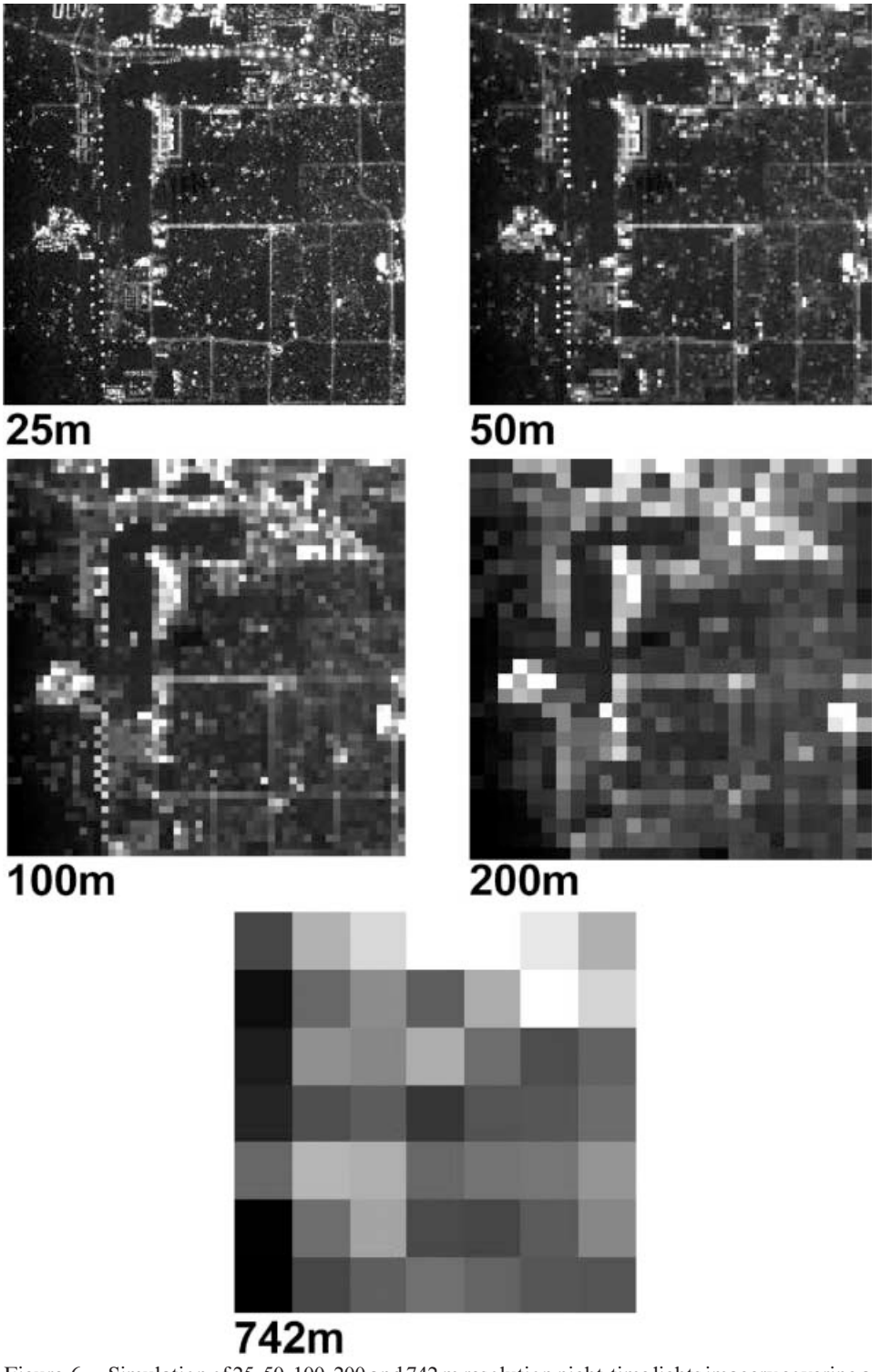

Figure 6. Simulation of 25, 50, 100, 200 and 742 m resolution night-time lights imagery covering a portion of Las Vegas, Nevada generated using the 1.5 m resolution image shown in figure 5. VIIRS low-light imagery will be at 742 m resolution, which is insufficient to discern urban morphology.

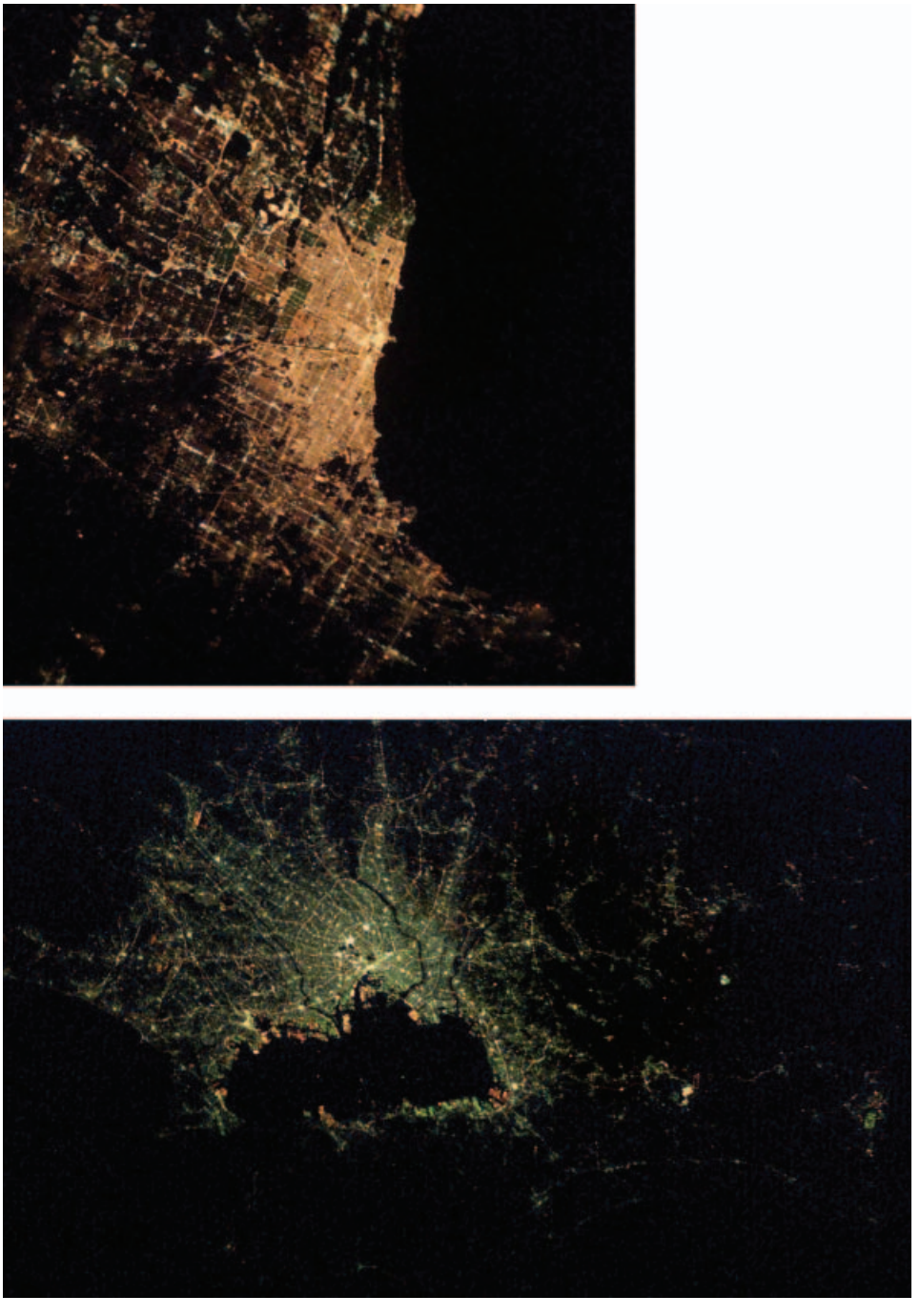

Figure 7. Chicago (top) and Tokyo (below) as imaged at night from the ISS. The resolution of the imagery is approximately 60 m. The ISS cities at night digital photography demonstrates the feasibility of collecting moderate resolution multispectral low-light imaging data globally from a satellite platform.

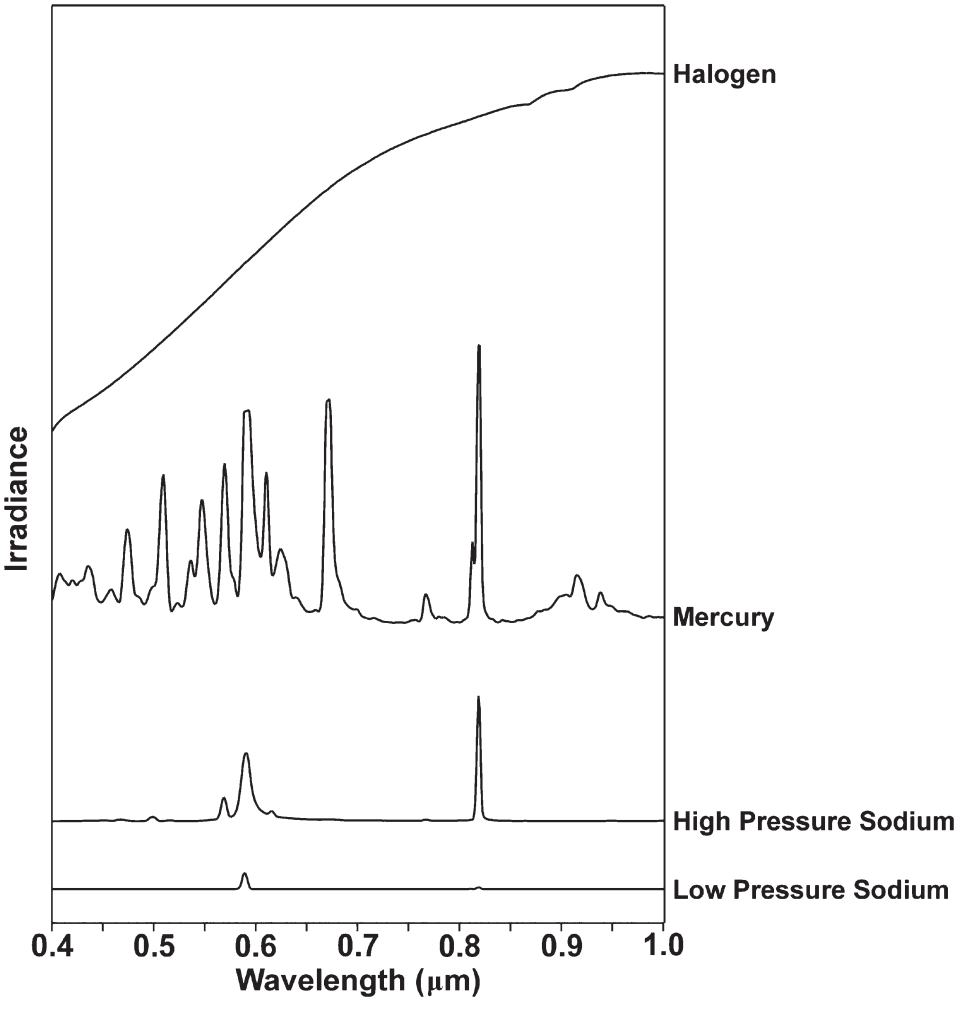

Figure 8. Field spectra of four different types of nocturnal lighting.

and sodium vapour lamps). Primary types of outdoor lighting used worldwide include incandescent, mercury vapour lamps, high pressure sodium vapour lamps, low pressure sodium vapour lamps, metal halide lamps and light-emitting diode (LEDs). The various types of light sources have distinctive spectral signatures (see figure 8).

There are several possible configurations and numbers of low-light spectral bands that should be considered for a future NightSat mission. The minimal configuration is for a single broad low-light imaging band designed to record radiances from a wide range of lighting types. A logical bandpass would be from 0.5 to 0.9 μm (commonly referred to as a panchromatic band), which could be designed, based on silicon detector technology and avoids the atmospheric scattering present in the blue part of the spectrum (0.4 to 0.5 μm) and the water absorption band centred at 0.95 μm. This is the spectral band used for low-light imaging on the DMSP-OLS and NPOESS-VIIRS. A NightSat with a single low-light imaging band, though producing less informative data, would have advantages in terms of a simpler

design, lower costs, and potentially lower data volume and simpler data processing for product generation.

Collecting data with a set of low-light imaging bands, specifically tailored for night-time lights, would be indispensable to (i) obtain quantities that can be related directly to international recognized measurements and standards for outdoor lighting, (ii) define the predominant type or mixture of lighting present, and consequently (iii) detect changes in lighting type over time. In considering the bandpass options for a multispectral Nightsat, it is important to consider the characteristics of human vision, internationally recognized lighting standards, the spectral content of lighting sources, and the responses of other species to different spectra.

With hyperspectral low-light imaging, the full spectral complexity of artificial light sources could be observed. This would be the best approach for the mapping of lighting types and how they change over time. Achieving the detection limits and spatial resolution requirements specified above with a hyperspectral imager, however, would be a technological challenge that would increase the sensor size, data rates, and processing complexity. Given the magnitude of these challenges, we propose that the first NightSat have from three to five low-light imaging bands.

Artificial night-time lighting design is based on the visual sensation of the human observer. The aim of photometry is to measure light in such a way that the result can be correlated with the visual sensation to a normal human observer exposed to that radiation. In 1979, Conference Generale des Poids et Mesures (CGPM 1979) redefined the basic SI unit candela (cd), formerly defined based on the radiation from platinum at the temperature of its solidification, as 'the luminous intensity, in a given direction, of a source that emits monochromatic radiation of frequency 540×10^{12} hertz and that has a radiant intensity in that direction of (1/683) Watt per steradian.' In redefining the candela, photometry merged with radiometry—a field commonly used in remote sensing. To achieve the aim of photometry, one must take into account the characteristics of human vision, i.e. its relative spectral responsivity. The relative luminous efficiency function for photopic vision—the photopic band—was originally proposed by Gibson and Tyndall (1923) and was adopted by the Commission International de l'Eclairage in 1924 (CIE 1924). The photopic band, shown in figure 9 has a bandpass (full width half maximum) spanning from 0.51 to 0.61 μm and has peak responsivity at 0.555 μm. Although the photopic band does not properly match the relative spectral responsivity of human vision (e.g. Judd 1951, Vos 1978, Stockman and Sharpe 1999) it has been widely adopted and remains an irrefutable standard in lighting science and technology. The photopic band has been published by Comité International des Poids et Mesures in 1982 (CIPM 1982) to supplement the 1979 definition of candela and republished by CIE in 2004 (CIE 2004). More recently, it has been adopted as an ISO standard (ISO 23539:2005). Photopic response is largely determined by the properties of the population of cone photoreceptors, which lie at the centre of the retinal region providing the most acute vision, the fovea. Night-time outdoor lighting has typical luminances (radiance in ISO photopic band) on the order of 1 to 2 cd/m^2. In this range of luminances, the vision response is derived mainly from cones. Because artificial night-time lighting installations are designed based on the photopic quantities (e.g. luminances) prescribed by standard rules or as required by customers, the photopic band is a key spectral band for NightSat applications such as estimation of ambient population, the spatial

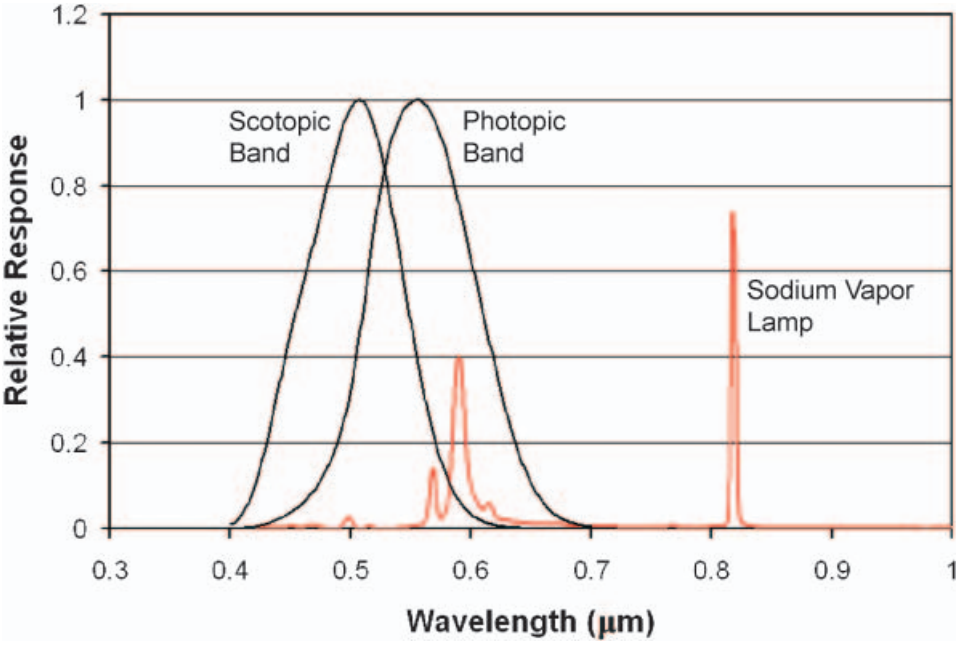

Figure 9. Relative response curves for the scotopic and photopic bands. For comparison, the spectrum from a high pressure sodium streetlight is plotted in red.

distribution of economic activity, and the measurement of development growth rates.

The spectral responsivity of human vision deviates significantly from the photopic response at very low levels of luminance when rod photoreceptors became more important than cones in determining the eye response. Vision with the retinal rods alone, at luminances under about 0.01 cd/m^2, is determined by the relative luminous efficiency function for scotopic vision (Le Grand 1951, Wyszecki and Stiles 1967). It was defined by CIE in 1951 (CIE 1951), recognized by CIPM in 1976 and 1982 (CIPM 1976, 1982), and adopted by ISO in 2005 (ISO 23539:2005). The term 'scotopic' should not be mistaken for 'night vision', which can involve both, rods and cones. It is much more restrictive because it applies to the rods alone. The scotopic vision generally occurs only in specific nocturnal situations recognizable because no colours are seen but only an achromatic whitish-greenish sensation. The scotopic band is the second standard band for physical photometry used in lighting engineering. The scotopic band, shown in figure 9, spans from 0.454 to 0.549 μm full width half maximum (FWHM) and has peak responsivity at 0.507 μm. The scotopic to photopic lumen ratio can be used to describe the whiteness of the light when more accurate chromaticity coordinates are not available. It is of particular interest for us because (i) the 'whiteness' of the light could be used as an additional estimator of parameters, such as population density and economic activity, (ii) the scotopic to photopic lumen ratio can be used to distinguish between the main class of lamp spectra (table 2), and (iii) the radiance in the scotopic band is fundamental to compute the effects of light pollution on the scotopic vision of the eye, i.e. for observers in low luminosity conditions. As an example, luminous stars tends to be seen with cones, in particular under bright skies, but pure, or almost pure, rod vision is responsible for the whitish starred sky that we see as background, in dark sites.

Table 2. Photopic versus scotopic lumen ratios for some outdoor lighting lamps.

Type of measured lamp	Scotopic vs. photopic lumen ratio
Low pressure sodium	0.21
35W high-pressure sodium	0.4
70W high-pressure sodium	0.55
100W high-pressure sodium	0.63
150W high-pressure sodium	0.68
250W high-pressure sodium	0.64
400W high-pressure sodium	0.67
80W HPL Mercury Vapour	1.18
125W incandescent	1.4
5W incandescent (2856K)	1.4
CIE Illuminant A (incandescent)	1.41
QTH halogen incandescent (3100K)	1.56
250W metal halide h	1.62
250W metal halide u	1.50
400W metal halide h	1.77
400W metal halide u	1.48
Warm-white fluorescent WW	0.97
Narrow band phosphor fluorescent (5000K)	1.96
Flat spectrum (calculated)	1.86
Blackbody 6600K	2.46
CIE D65 (solar standard spectrum) (Moon)	2.46

Based on these considerations, the scotopic band should be included with the photopic band on a multispectral Nightsat.

For improved discrimination of lighting types and changes in lighting types over time, additional low-light imaging bands at wavelengths longer than the photopic band could be defined. These additional low-light imaging bands would assist in discrimination of lighting types with broad spectral emission, like incandescent (see figure 8), metal halide (flat broad spectra) and LED lamps. Radiance emissions from incandescent lamps and flames follow a blackbody emission pattern and are much brighter in the near infra-red (NIR) than in the visible. In contrast, emissions from LED lamps are typically low in the NIR. There is a prominent sodium vapour emission line at 0.82 μm (see figure 8) for which a spectral band could be tailored.

To resolve the questions raised on the number of spectral bands that would be required to discriminate major lighting types from space, we have examined a set of colour images acquired from the ISS. Figure 7 shows images from Chicago and Tokyo. The orange lighting observed across most of Chicago arises from the prominence of sodium vapour lights in many American cities. The greenish appearing lights found in some neighbourhoods of Chicago are owing to mercury vapour lamps. The lights in the Tokyo image are nearly all green, indicating the widespread use of mercury vapour lamps. There are several shipyards on Tokyo Bay lit with sodium vapour lamps.

The evidence from the ISS photography and the ability to separate lighting types, based on the scotopic and photopic band (table 2), indicates that it would be possible to distinguish major lighting types and changes in lighting type using three low light imaging bands. For a system with three low-light imaging spectral bands, we recommend: (a) the scotopic band from 0.454 to 0.549 μm, (b) the photopic band from 0.51 to 0.61 μm and (c) a broad red and near-infrared band spanning from 0.61 to 0.9 μm. Improvements in the spectral discrimination of lighting types could be

Table 3. Spectral band options for panchromatic, three, four and five low-light imaging bands.

Number of bands	Band 1	Band 2	Band 3	Band 4	Band 5
One	0.5–0.9 um				
Two	Not recommended				
Three	Scotopic band 0.454 to 0.549 μm	Photopic band 0.51 to 0.61 μm	Red to NIR band 0.61 to 0.9 μm		
Four	Scotopic band 0.454 to 0.549 μm	Photopic band 0.51 to 0.61 μm	Red band 0.61 to 0.7 μm	NIR band 0.7 to 0.9 μm	
Five	Scotopic band 0.454 to 0.549 μm	Photopic band 0.51 to 0.61 μm	Red band 0.61 to 0.7 μm	NIR band A 0.7 to 0.8 μm	NIR band B 0.8 to 0.9 μm

achieved by splitting this third band into either two or three individual bands. The recommended four band system would have the scotopic, photopic, red and broad NIR bands. The recommended five band system would split the broad NIR band into two, with the fifth band encompassing the prominent sodium vapor emission line present at 0.82 These options are presented in table 3.

5.3 *Low light imaging detection limits*

In examining the Cirrus camera imagery, we found that the dimmest detectable lighting had radiances in the range of $5E^{-5}$ Watts cm^{-2} sr^{v1} μm^{-1}. These areas were generally lit terrain closely surrounding shielded lights. The signal-to-noise ratio (SNR) for this lighting was about nine. Lighting from individual poorly shielded 100-Watt incandescent bulbs present on the exteriors of recently constructed homes produced measured radiances in the range of $1E^{-4}$ Watts cm^{-2} sr^{-1} μm^{-1} The Cirrus camera saturated at radiances above $3.83E^{-3}$ Watts cm^{-2} sr^{-1} μm^{-1}. The Luxor light (figure 4) produced a 37 m diameter circular zone of saturated pixels. Other small areas of saturated data were found on large casinos near the Luxor. Since the Luxor beacon is the brightest light on earth, this effectively defines the saturation radiance for a Nightsat at approximately $2.5E^{-2}$ Watts cm^{-2} sr^{-1} μm^{-1}, a level suitable for daylight imaging of the earth.

The night-time light features from the Cirrus camera imagery were compared against 1 m Ikonos imagery acquired a week earlier. This examination revealed that the Cirrus camera imagery detected lighting in most, but not all, areas of development. The Cirrus camera was unable to detect lit surfaces more than about 10 m out from individual streetlights. Examining the background DN (digital number) values along transects from dark desert areas through the centre of the Las Vegas Strip revealed that the Cirrus camera was unable to detect the broad region of terrain lit by artificial night sky brightness inside of an urban centre. Likewise, the Cirrus camera would have been unable to detect moonlit terrain if the data had been collected under full moon conditions.

There is a growing trend for the installation of shielding on outdoor lighting, to reduce light pollution and to conserve energy. Full cutoff shielding directs all of the lighting towards the surface below, with no lighting emissions directed towards the sky. It would be important to be able to detect the areas lit by well shielded lighting installations out to illumination levels commonly prescribed for outdoor lighting. Otherwise, implementation of currently available technology and continuation of

the trend towards shielding could render a NightSat useless for the detection of widespread artificial lighting.

From these observations, it is evident that are several detection limit options for a NightSat sensor. The detection of lighting from commercial centres and streetlights as widely configured today could be accomplished with a system having capabilities comparable to the Cirrus digital camera system (DCS) camera, i.e. in the $1E^{-5}$ Watts cm^{-2} sr^{-1} μm^{-1} range for the photopic band. Because the Cirrus camera was unable to detect many areas of known lighting, it is recommended that the Nightsat detection limits be substantially lower than those achieved by the Cirrus camera. It is estimated that detection of the terrain lit by shielded lights and sparse lighting in rural environments would require detection limits in the $2.5E^{-8}$ Watts cm^{-2} sr^{-1} μm^{-1} range in photopic band for a 50 m pixel size. Quantification of lighting levels on terrain illuminated by artificial sky brightness in and around urban centres would require detection limits in the $5E^{-10}$ Watts cm^{-2} sr^{-1} μm^{-1} range in photopic band.

Based on these considerations we recommend the Nightsat's minimal detectable average spectral radiance in photopic band at $2.5E^{-8}$ Watts cm^{-2} sr^{-1} μm^{-1} with a SNR of 10 and a saturation radiance of $2.5E^{-2}$ Watts cm^{-2} sr^{-1} μm^{-1}. This saturation radiance would make it possible for Nightsat to collect unsaturated data, even during the daylight portion of the orbits. If a detection limit of $5E^{-10}$ Watts cm^{-2} sr^{-1} μm^{-1} could be achieved, it would be possible to analyse the patterns of artificial sky brightness that surround major cities. Given the engineering challenge of achieving the recommended detection limits, it is clear that systems capable of detecting light in the $2.5E^{-8}$ Watts cm^{-2} sr^{-1} μm^{-1} range would provide quite useful data.

The question then arises, at what detection limit would a Nightsat begin to have a capability to detect moonlit terrain? How would this affect the data quality and processing of Nightsat data acquired under high lunar illumination conditions? Lunar illuminance depends mainly on the phase, the elevation of the moon above the horizon, and atmospheric extinction. We can roughly calculate the magnitude order of the maximum radiance observed from the satellite for a typical soil (20% albedo) near full moon (0.3 lx), and an atmospheric transmission of 0.7. This radiance is estimated to be $2E^{-8}$ Watts cm^{-2} sr^{-1} μm^{-1} in the photopic band. By setting the Nightsat detection limits slightly above the sensitivity required to detect heavily moonlit objects, the effects of lunar cycles on the Nightsat observations would be reduced. For a sensor capable of detecting radiances in the $5E^{-10}$ Watts cm^{-2} sr^{-1} μm^{-1} range observations of dimly lit terrain would have non-negligible errors, if measured during moonlight. The observed radiance of moonlighted soil is comparable to the minimal radiance required to observe a dimly lit road, even if the ratio between the luminances of the road and the soil is around 15. In fact, a typical 8 m wide road fills 1/6 of a pixel with 50 m pixel size and it likely has a uniformity of about 50%, whereas moonlight has a filling factor of 100% and a uniformity of 100%. The lunar contribution could not be computed and subtracted, unless detailed information about surface reflectance was available at the resolution of the Nightsat data. In the absence of surface albedo, valid radiances could be extracted from the upper end of the dynamic range (e.g. above $1E^{-6}$ Watts cm^{-2} sr^{-1} μm^{-1}), thresholding out the dim lighting associated with moonlit terrain. With this lunar thresholding approach, there would be some loss in the detection of dim lighting associated sparse rural and exurban populations when

lunar illuminance is high. It is clear that as with the OLS, the best night-time lights data would be collected on nights with little or no lunar illuminance.

5.4 *Thermal band*

Thermal band data would be essential for discrimination of cloud-free areas observed with a NightSat. In addition, thermal band data would facilitate in the identification of lighting produced from combustion (e.g. biomass burning and gas flares). The thermal band data could be provided from another sensor, if NightSat were flown on a multisensor platform. Otherwise, a NightSat would need to have at least one thermal band for use in cloud and fire discrimination. An examination of MODIS Airborne Simulator data collected over Los Angeles, California, indicates that a single thermal band in the 3 to 5 μm region could be used for both, cloud and fire. The thermal band data should be co-registered with the low-light imaging band data, but the spatial resolution could be somewhat coarser, perhaps in the 300 to 500m range.

5.5 *Orbital requirements*

There are four primary issues to be considered for the orbit of a future NightSat mission.

5.5.1 Global coverage. The orbit should permit the collection of global coverage from a single satellite. Achieving global coverage with a single satellite could only be accomplished using a polar orbit.

5.5.2 Overpass time. Having a consistent overpass time would be important for accurate change detections. In many regions of the world, outdoor lighting is gradually turned off starting around 10 p.m. Thus, the ideal overpass time would be the middle of the evening, i.e. in the 8:30 to 10:00 p.m. range. This time slot would permit the observation of the maximum extent of lighting in regions where lights may be gradually turned off as midnight approaches. An earlier overpass time would result in reductions in data coverage, due to solar contamination present at mid-to-high latitudes during the summer months. As with the requirement for global coverage, the requirement for a consistent overpass time implies a polar orbit.

5.5.3 Low altitude. Achieving the spatial resolution and detection limit targets defined above will require a specialized sensor, capable of collecting and processing minute quantities of light. This would be easier—in terms of the sizing of the sensor—from a lower altitude orbit than a higher altitude orbit.

5.5.4 Repeat cycle. Multiple collections would be required for most parts of the world to ensure that a global cloud-free annual composite could be produced. The other factor to consider is the lunar cycle. Automated extraction of surface lighting features would become complicated for a sensor capable of detecting moonlit terrain (e.g. detection limits in the range of $2E^{-8}$ Watts cm^{-2} sr^{-1} μm^{-1}). For example, shadows would appear in the imagery where terrain or large buildings obstructed moonlight. The lunar contribution to the signal and variations introduced by shadowing would detract from the quality of NightSat data collected on nights when lunar illumination is high. Therefore, it would be important to randomize the mix of lunar conditions under which observations would occur during a year for any particular location. The least desirable repeat cycle for a Nightsat would be 29 days,

matching the synodic period of the Moon (29.5305 89 days on average). With this type of orbit, orbital strips would be acquired at nearly the same lunar phase throughout the year. Likewise, a repeat cycle period of 15 days would result in the collection of data at two opposite lunar phases throughout the year. To better randomize the lunar illumination conditions of collections for each part of the world during a year, a repeat cycle of ~20 days could be utilized. With a polar orbit and a 20-day repeat cycle, most areas of the world could be collected 18 times per year.

5.5.5 Alternative orbits. A polar orbit would be required to achieve global coverage from a single satellite and a consistent overpass time in the early evening. A Nightsat instrument on a platform, such as the ISS, could acquire substantial quantities of valuable night-time lights data. The relatively low orbit of the ISS would make achieving the GSD and radiometric capabilities specified easier. The latitude range over which data could be collected would be limited to approximately 50° north and south. Users would need to consider how variations in the local overpass times might affect the observations. More detailed analysis of the diurnal pattern of night-time lighting and power outages associated with disasters could be observed from geostationary satellites. Because geostationary orbits are much higher than standard polar orbits, the spatial resolutions would be coarse. However, as seen with the OLS, spatial resolutions in the range of 1 to 5 km would still provide useful data on diurnal patterns and power outages.

6. Nightsat observational requirements

We propose a mission sensor with similarity to Landsat, optimized for the construction of annual global cloud-free, radiance-calibrated composite images of night-time lights. The system capabilities are summarized in table 4.

(1) Low-light imaging with one or more visible/NIR bands with detection limits and dynamic range suitable for detecting and measuring radiances from night-time lights. The minimal detectable radiance should be at least $2.5E^{-8}$ Watts $cm^{-2}sr^{-1}\mu m^{-1}$.
(2) Nadir pointing with a GSD in the 50 to 100 m range, and a swath of approximately 100 km.

Table 4. Nightsat performance metrics.

	Low-light band(s)	Thermal band(s)
Ground sample distance (m)	50–100	300–500
GIFOV (m)	70–150	400–600
Swath (km)	~200	~200
Revisit time (days)	~20	~20
Geolocation error (RMS in m)	50	100
Min. radiance or temperature (Watts $cm^{-2}sr^{-1}\mu m^{-1}$ or degrees K)	Good: $2.5E^{-8}$ (human settlements) Better: $2.5E^{-9}$ (terrain lit by shielded lighting and sparsely lit development) Best: $5E^{-10}$ (artificial sky brightness)	240 K
Max. radiance or temperature (Watts $cm^{-2}sr^{-1}\mu m^{-1}$ or degrees K)	$2.5E^{-2}$ (sunlit terrain)	400 K
Duty cycle	40%	40%

(3) On-board calibration or a repeatable procedure for calibrating sensor data to radiance units.
(4) One or more thermal bands for detecting cloud-free areas and contamination by fires (300 to 500 m GSD). The VIIRS instrument could provide the thermal band data if NightSat were flown on an NPOESS satellite.
(5) Collection from a polar orbiting satellite in low earth orbit, with a mid-evening overpass (8:30 to 10:00 p.m. local time) and a repeat cycle of about 20 days.
(6) Geolocation accuracy comparable to Landsat.

7. Conclusion

Satellite sensors, designed for the collection of reflected sunlight, do not have detection limits low enough to observe nocturnal lighting. Satellite observation of night-time lights at a spatial resolution, suitable for mapping urban forms and detection, limits tailored to span the range from sparse development in rural areas to the cores of urban centres will require a specialized sensor. We have analysed a combination of field, laboratory, and airborne data to develop the general specifications for such a system, which we call Nightsat. The data from a Nightsat system would enable a wide range of social, economic, and biological applications where there is currently a dearth of systematically collected, unbiased, global data. Nightsat data would provide important constraints and inputs for the spatial modelling of human population growth and distribution, land use, rates of development, anthropogenic emissions to the atmosphere and independent estimation of economic indices. In addition, Nightsat data would be used to model and understand human impacts on the environment such as the proliferation of impervious surface area, non-point sources of aquatic pollution, habitat fragmentation, and the direct effects of nocturnal lighting on night environment, human health, security, and the visibility of stars.

Moderate resolution low-light imaging sensor data would be an important complement to the mapping capacity of moderate resolution daytime imaging sensors such as Aster and Landsat because it would provide an unambiguous indication of the presence of development and growth in development. Nightsat data would also be useful for calibrating and validating coarser resolution low-light imaging data acquired with the OLS and VIIRS sensors.

To be effective in delineating primary night-time lighting patterns, Nightsat low-light imaging data must be acquired in the range of 50 to 100 m spatial resolution and achieve minimal detectable radiances in the range of $2.5E^{-8}$ Watts cm^{-2} sr^{-1} μm^{-1} (or better) with a SNR of 10. While panchromatic low-light imaging data would be useful, multispectral low-lighting imaging data acquired with three to five spectral bands would enable more quantitative applications and enable the detection of lighting type conversions. Cloud and fire screening of the low light imaging data would be accomplished using simultaneously acquired thermal band data. The thermal band data could come from VIIRS if Nightsat were flown on an NPOESS satellite. The system would use a combination of methods to produce radiance-calibrated data. Geolocation accuracy would be $\sim$50 m, comparable to that of Landsat. The system objective would be to collect a sufficient quantity of imagery to construct annual global cloud-free composites of night-time lights. A near-sun-synchronous polar orbit, with an early evening overpass, would provide temporal consistency important

for change detection. The overall system performance is listed in table 4. It should be noted that additional research would be required to optimize the detection limits for each of the proposed low-light imaging bands based on the spectra of a wide range of currently available lighting types.

The weight of scientific evidence over the past decades point to human activity as the primary driver for environmental and biological change on the planet. This is true for the land, the sea, and the atmosphere. While other satellite missions focus on observing the changes in the environment, the Nightsat mission will focus on mapping the spatial distribution and intensity of an indicator of human activity—artificial lighting. The Nightsat sensor requirements have been set to cover a wide range in brightness levels and lighting types, providing detection of sparse development in rural areas and detailed mapping of forms present in urban areas. The ability to track the growth in lighting globally, in a consistent manner on an annual basis would enable a synoptic understanding of the human footprint on the land and ocean surface.

References

BALK, D., POZZI, F., YETMAN, G., DEICHMANN, U. and NELSON, A., 2005, The distribution of people and the dimension of place: methodologies to improve the global estimation of urban extent. *Proceedings of the Urban Remote Sensing Conference*, Tempe, Arizona, April 2005.

CHO, K., R. Ito. R., SHIMODA, H. and SAKATA, T., 1999, Fishing fleet lights and sea surface temperature distribution observed by DMSP/OLS sensor. *International Journal of Remote Sensing*, **20**, pp. 3–9.

CIE 1924, *Commission Internationale de l'Éclairage C.I.E.*, Compte Rendu des Séances, Sixième Session, Genève 1924, p. 67.

CIE 1951, *Commission Internationale de l'Éclairage C.I.E.*, Compte Rendu, CIE Central Bureau, vol. 3, Table 11, pp. 37–39.

CIE 2004, The CIE system of physical photometry, CIE Standard 010/E: 2004.

CINZANO, P., FALCHI, F., ELVIDGE, C.D. and BAUGH, K.E., 2000, The artificial night sky brightness mapped from DMSP Operational Linescan System measurements. *Monthly Notices of the Royal Astronomical Society*, **318**, pp. 641–657.

CINZANO, P., FALCHI, F. and ELVIDGE, C.D., 2001a, Naked eye star visibility and limiting magnitude mapped from DMSP-OLS satellite data. *Monthly Notices of the Royal Astronomical Society*, **323**, pp. 34–46.

CINZANO, P., FALCHI, F. and ELVIDGE, C.D., 2001b, The first world atlas of the artificial night sky brightness. *Monthly Notices of the Royal Astronomical Society*, **328**, pp. 689–707.

CINZANO, P. and ELVIDGE, C.D., 2004, Night sky brightness at sites from DMSP-OLS satellite measurements. *Monthly Notices of the Royal Astronomical Society*, **353**, pp. 1107–1116.

CIPM 1976, Comité Internationale Des Poids et Mesures C.I.P.M., Proces-Verbaux, 44, p. 4.

CIPM 1982, Comité Consultatif de Photometrie et Radiometrie, Session-1982, Bureau International Des Poids et Mesures, Sevres, France.

CGPM 1979, Comptes Rendus des Seances de la 16e Conference Genrale des Poids et Mesures, Paris 1979, Bureau International Des Poids et Mesures, Sevres, France.

DOBSON, J., BRIGHT, E.A., COLEMAN, P.R., DURFEE, R.C. and WORLEY, B.A., 2000, LandScan: a global population database for estimating populations at risk. *Photogrammetric Engineering and Remote Sensing*, **66**, pp. 849–857.

DOLL, C.N.H., MULLER, J.-P. and ELVIDGE, C.D., 2000, Night-time imagery as a tool for global mapping of socio-economic parameters and greenhouse gas emissions. *Ambio*, **29**, pp. 157–162.

Ebener, S., Murray, C., Tandon, A. and Elvidge, C., 2005, From wealth to health: modeling the distribution of income per capita at the sub-national level using night-time lights imagery. *International Journal of Health Geographics*, **4**, pp. 5–14.

Elvidge, C.D., Baugh, K.E., Kihn, E.A., Kroehl, H.W. and Davis, E.R., 1997a, Mapping city lights with nighttime data from the DMSP Operational Linescan System. *Photogrammetric Engineering and Remote Sensing*, **63**, pp. 727–734.

Elvidge, C.D., Baugh, K.E., Hobson, V., Kihn, E., Kroehl, H., Davis, E. and Cocero, D., 1997b, Satellite inventory of human settlements using nocturnal radiation emissions: a contribution for the global toolchest. *Global Change Biology*, **3**, pp. 387–395.

Elvidge, C.D., Baugh, K.E., Hobson, V.R., Kihn, E.A. and Kroehl, H.W., 1998, Detection of fires and power outages using DMSP-OLS data. In *Remote Sensing Change Detection: Environmental Monitoring Methods and Applications*, R. Lunetta and C. Elvidge (Eds), pp. 123–135 (Ann Arbor Press).

Elvidge, C.D., Baugh, K.E., Dietz, J.B., Bland, T., Sutton, P.C. and Kroehl, H.W., 1999, Radiance calibration of DMSP-OLS low-light imaging data of human settlements. *Remote Sensing of Environment*, **68**, pp. 77–88.

Elvidge, C.D., Imhoff, M.L., Baugh, K.E., Hobson, V.R., Nelson, I., Safran, J., Dietz, J.B. and Tuttle, B.T., 2001, Night-time lights of the world: 1994–1995. *ISPRS Journal of Photogrammetry and Remote Sensing*, **56**, pp. 81–99.

Elvidge, C.D., Milesi, C., Dietz, J.B., Tuttle, B.T., Sutton, P.C., Nemani, R. and Vogelmann, J.E., 2004, U.S. Constructed Area Approaches the Size of Ohio. *AGU EOS Transactions*, **85**, p. 233.

Gibson, K.S. and Tyndall, E.P.T., 1923, Visibility of radiant energy. *Scientific Papers of the Bureau of Standards*, **19**, pp. 131–191.

Hansen, J., 2001, Light at night, shiftwork, and breast cancer risk. *Journal of the National Cancer Institute*, **93**, pp. 1513–1515.

Imhoff, M.L., Lawrence, W.T., Elvidge, C.D., Paul, T., Levine, E., Privalsky, M.V. and Brown, V., 1997, Using nighttime DMSP/OLS images of city lights to estimate the impact of urban land use on soil resources in the United States. *Remote Sensing of Environment*, **59**, pp. 105–117.

Imhoff, M.L., Bounoua, L., Defries, R., Lawrence, W.T., Stutzer, D., Tucker, C.J. and Rickett, T., 2004, The consequences of urban land transformation on net primary productivity in the United States. *Remote Sensing of Environment*, **89**, pp. 434–443.

ISO 2005, *The CIE system of physical photometry, ISO Standard 23539:2005(E)* (Geneva: International Organization for Standardization).

Judd, D.B., 1951, Report of U.S. Secretariat Committee on Colorimetry and Artificial Daylight. *Proceedings of the Twelfth Session of the CIE, Stockholm*, pp. 1–11 (Paris: Bureau Central de la CIE).

Lee, T.F., Miller, S.D., Turk, F.J., Schueler, C., Julian, R., Deyo, S., Dills, P. and Wang, S., 2006, The NPOESS/VIIRS day/night visible sensor. *Bulletin of the American Meteorological Society*, **87**, pp. 191–199.

Le Grand, Y., 1951, Comité d'Études sur la Lumière et la Vision. In *Commission Internationale de l'Éclairage C.I.E., Compte rendu Stockholm*, Vol. 1, Chap. 4, p. 1.

Longcore, T. and Rich, C., 2004, Ecological light pollution. *Frontiers in Ecology and the Environment*, **2**, pp. 191–198.

Maxwell, M.R., Henry, A., Elvidge, C.D., Safran, J., Hobson, V.R., Nelson, I., Tuttle, B.T., Dietz, J.B. and Hunter, J.R., 2004, Fishery dynamics of the California market squid (*Loligo opalescens*), as measured by satellite remote sensing. *Fishery Bulletin*, **102**, pp. 661–670.

Milesi, C., Elvidge, C.D., Nemani, R.R. and Running, S.W., 2003, Assessing the impact of urban land development on net primary productivity in the southeastern United States. *Remote Sensing of Environment*, **86**, pp. 273–432.

MILESI, C., ELVIDGE, C.D., DIETZ, J.nB., TUTTLE, B.J., NEMANI, R.R. and RUNNING, S.W., 2005, Mapping and modeling the biogeochemical cycling of turf grasses in the United States. *Environmental Management*, **36**, pp. 426–438.

MILLER, S.D., HADDOCK, S.H.D., ELVIDGE, C.D. and LEE, T.F., 2005, Detection of a bioluminescent milky sea from space. *Proceedings of the National Academy of Sciences*, **102**, pp. 14181–14184.

PAULEY, S.M., 2004, Lighting for the human circadian clock: recent research indicates that lighting has become a public health issue. *Medical Hypotheses*, **63**, pp. 588–596.

RICH, C., and LONGCORE, T. (Eds), 2006, *Ecological Consequences of Artificial Night Lighting* (Washington, D.C.: Island Press).

RODHOUSE, P.G., ELVIDGE, C.D. and TRATHAN, P.N., 2001, Remote sensing of the global light-fishing fleet: an analysis of interactions with oceanography, other fisheries and predators. *Advances in Marine Biology*, **39**, pp. 261–303.

SALMON, M., 2006, Protecting sea turtles from artificial night lighting at Florida's oceanic beaches. In *Ecological Consequences of Artificial Night Lighting*, C. Rich and T. Longcore (Eds), pp. 141–168 (Washington, D.C.: Island Press).

SALMON, M., WITHERINGTON, B.E. and ELVIDGE, C.D., 2000, Artificial lighting and the recovery of sea turtles. In *Sea Turtles of the Indo-Pacific: Research, Management and Conservation*, N. Pilcher and G. Ismail (Eds), pp. 25–34 (London: ASEAN Academic Press).

SAXON, E.C., PARRIS, T. and ELVIDGE, C.D., 1997, Satellite Surveillance of National CO2 Emissions From Fossil Fuels. Harvard Institute for International Development, Development Discussion Paper 608.

SMALL, C., 2005, Global analysis of urban reflectance. *International Journal of Remote Sensing*, **26**, pp. 661–681.

SMALL, C., POZZI, F. and ELVIDGE, C., 2005, Spatial analysis of global urban extent from DMSP-OLS night lights. *Remote Sensing of Environment*, **96**, pp. 277–291.

STEVENS, R.G. and REA, M.S., 2001, Light in the built environment: potential role of circadian disruption in endocrine disruption and breast cancer. *Cancer Causes and Control*, **12**, pp. 279–287.

STOCKMAN, A. and SHARPE, L.T., 1999, Cone spectral sensitivities and color matching. In *Color Vision: From Genes to Perception*, K. Gegenfurtner and L.T. Sharpe (Eds) pp. 51–85 (Cambridge: Cambridge University Press).

SUTTON, P., 1997, Modeling population density with nighttime satellite imagery and GIS. *Computers, Environment, and Urban Systems*, **21**, pp. 227–244.

SUTTON, P.C., 2003, A scale-adjusted measure of "urban sprawl" using nighttime satellite imagery. *Remote Sensing of Environment*, **86**, pp. 353–363.

SUTTON, P., ROBERTS, D., ELVIDGE, C.D. and MEIJ, J., 1997, A comparison of nighttime satellite imagery and population density for the continental United States. *Photogrammetric Engineering and Remote Sensing*, **63**, pp. 1303–1313.

SUTTON, P.C., ROBERTS, D., ELVIDGE, C. and BAUGH, K., 2001, Census from heaven: an estimate of the global population using nighttime satellite imagery. *International Journal of Remote Sensing*, **22**, pp. 3061–3076.

SUTTON, P.C., ELVIDGE, C. and OBREMSKI, T., 2003, Building and evaluating models to estimate ambient population density. *Photogrammetric Engineering and Remote Sensing*, **69**, pp. 545–553.

TOENGES-SCHULLER, N., STEIN, O., ROHRER, F., WAHNER, A., RICHTER, A., BURROWS, J.P., BEIRLE, S., WAGNER, T., PLATT, U. and ELVIDGE, C.D., 2006, Global distribution patter of anthropogenic nitrogen oxide emissions: Correlation analysis of satellite measurements and model calculations. *Journal of Geophysical Research*, **111**, p. D05312.

VOGELMANN, J.E., HOWARD, S.M., YANG, L., LARSON, C.R., WYLIE, B.K. and VAN DRIEL, N., 2001, Completion of the 1990s national land cover data set for the

conterminous united states from landsat thematic mapper data and ancillary data sources. *Photogrammetric Engineering and Remote Sensing*, **67**, pp. 650–662.

VOS, J.J., 1978, Colorimetric and photometric properties of a 2-deg fundamental observer. *Color Research and Application*, **3**, pp. 125–128.

WALUDA, C.M., TRATHAN, P.N., ELVIDGE, C.D., HOBSON, V.R. and RODHOUSE, P.G., 2002, Throwing light on straddling stocks of *Ilex argentinus*: assessing fishing intensity with satellite imagery. *Canadian Journal of Fisheries and Aquatic Sciences*, **59**, pp. 592–596.

WEEKS, J.R., 2004, Using remote sensing and geographic information systems to identify the underlying properties of urban environments. In *New Forms of Urbanization: Conceptualizing and Measuring Human Settlement in the Twenty-first Century*, T. Champion and G. Hugo (Eds) (London: Ashgate Publishing Limited).

WEEKS, J.R., LARSON, D. and FUGATE, F., Patterns of urban land use as assessed by satellite imagery: an application to Cairo, Egypt. In *Population, Land Use, Environment: Research Directions*,B. Entwisle, R. Rindfuss and P. Stern (Eds) (Washington, D.C.: National Research Council). In press.

WYSZECKI, G. and STILES, W.S., 1967, *Color Science* (New York: John Wiley).